# Using Digital Aerial Photogrammetry and the Random Forest Approach to Model Forest Inventory Attributes in Beech- and Spruce-dominated Central European Forests

CHRISTOPH STRAUB & CHRISTOPH STEPPER, Freising

**Keywords**: Digital aerial photographs, semi-global matching, canopy height model, random forest, forest inventory

**Summary:** Surface models generated using dense image matching of aerial photographs have potential for use in the area-based prediction of forest inventory attributes. Few studies have examined the impact of the forest type on the performance of models used to predict forest attributes. Moreover, with regard to central European forests, little is known about how accurately attributes other than volume and basal area can be estimated using image-based surface models. Thus, in this study, we assessed the accuracy of such estimates for five forest attributes – stem density *N*, basal area *G*, quadratic mean diameter *QMD*, volume *V*, and Lorey's mean height $H_L$ – for a beech- and a spruce-dominated forest in northern Bavaria, Germany. These estimates were made using a workflow combining data from aerial photographs obtained from regularly scheduled surveys and field plot measurements from periodic forest inventories conducted in Bavarian state forests. Semi-Global Matching was used to derive surface models from the air photos which were normalized with terrain models from airborne laser scanning to derive canopy height models (CHM). Based on the CHM values at the respective field plots, a set of 14 predictor variables characterizing tree height distribution was computed. For the prediction, individual random forest models were trained and cross-validated separately for both test sites. With respect to relative *RMSEs*, i.e., divided by the observation means, most distinct differences were observed for the prediction of *QMD* with a slightly higher level of accuracy for the spruce-dominated forest. Best results were achieved for $H_L$, while poorest model performances were obtained for *N*. The relative plot-level *RMSEs* for *N*, *G*, *QMD*, *V*, and $H_L$ were: 70.3%, 36.0%, 32.3%, 37.8%, and 12.4% for the beech-dominated and 74.9%, 35.2%, 24.9%, 33.3%, and 12.4% for the spruce-dominated forest. Thus, with the exception of *QMD*, the forest type did not considerably influence the model accuracies.

**Zusammenfassung:** *Verwendung von photogrammetrischen Oberflächenmodellen und Random Forest zur Modellierung forstlicher Kenngrößen in buchen- und fichtendominierten Wäldern in Mitteleuropa.* Aus Stereo-Luftbildern abgeleitete Oberflächenmodelle können für die flächige Modellierung forstlicher Kenngrößen verwendet werden. Bisher wurde der Einfluss des Waldtyps auf die Genauigkeit der Modellierung nur in wenigen Studien untersucht. Außer für die Kenngrößen Holzvolumen und Grundfläche gibt es für mitteleuropäische Wälder bisher wenig Erfahrung, mit welcher Genauigkeit forstliche Kennwerte mit bildbasierten Oberflächenmodellen modelliert werden können. Deshalb wurde in dieser Studie die Modellierungsgenauigkeit für fünf verschiedene forstliche Inventurmerkmale untersucht – Stammzahl *N*, Grundfläche *G*, quadratischer Mitteldurchmesser *QMD*, Volumen *V* und Lorey'sche Mittelhöhe $H_L$ – sowohl für eine buchendominierte als auch für eine fichtendominierte Untersuchungsfläche im Norden von Bayern. Hierfür wurde ein Arbeitsablauf angewendet, der regelmäßig erhobene amtliche Luftbilder mit terrestrischen Stichprobenmessungen einer Forstbetriebsinventur in bayerischen Staatswaldflächen kombiniert. Die Berechnung von Oberflächenmodellen aus den Luftbildern erfolgte mittels Semi-Global Matching, welche zur Ableitung von Kronenhöhenmodellen (KHM) mit einem Geländemodell aus Laserscannermessung normalisiert wurden. Auf Grundlage der KHM wurden an den Stichprobenkreisen der Forstbetriebsinventur 14 Prädiktorvariablen zur Charakterisierung der Höhenverteilung abgeleitet. Für die Schätzung wurden einzelne Random Forest Modelle jeweils getrennt für beide Untersuchungsgebiete trainiert und validiert. Bezogen auf relative *RMSEs*, d.h. normalisiert mit dem Mittelwert der Beobachtungen, wurden die deutlichsten Unterschiede für die Schätzung des *QMD* festgestellt, mit einer etwas besseren Genauigkeit für die fichtendominierte Fläche. Die besten Ergebnisse wurden für die Modellierung der $H_L$ erzielt, wohingegen die geringsten

Genauigkeiten für *N* festgestellt wurden. Auf Inventurkreisebene wurden die folgenden relativen *RMSEs* für *N*, *G*, *QMD*, *V*, und $H_L$ berechnet: 70.3%, 36.0%, 32.3%, 37.8%, und 12.4% für die buchendominierte Fläche und 74.9%, 35.2%, 24.9%, 33.3%, und 12.4% für den fichtendominierten Wald. Mit Ausnahme für den *QMD* hatte der Waldtyp demnach keinen maßgeblichen Einfluss auf die Genauigkeit der Modelle.

## 1 Introduction

Quantitative estimates of certain forest inventory attributes, such as mean tree height or timber volume per hectare, are crucial for sustainable forest management practice. At present, state forests in Bavaria, Germany, which account for 30% of the total forest area in Bavaria (THÜNEN-INSTITUT 2015), are inventoried once every 10 years by the Bavarian State Forest Enterprise (BaySF) to gain quantitative information about the current state and future development of the forest. In 2015, the BaySF conducted such inventories for 73,805 hectares, i.e., 10.2% of the total state forest area (BAYSF 2015). As fieldwork is time-consuming and labour-intensive, terrestrial measurements are restricted to sample plots which are distributed systematically across the state forests based on a regular 200 m × 200 m grid. The field inventories are designed for evaluations at the forest enterprise level for which characteristic values of specific forest attributes can be estimated based on statistical evidence. These key figures are very valuable for strategic planning purposes. However, information for forest stand regions, which are the smallest management units, cannot be deduced from these data. Thus, in order to support operational planning and monitoring, higher resolution information about the spatial distribution of forest characteristics, which cannot be provided by the sample plot measurements alone, would be beneficial.

Remote sensing can support such terrestrial forest inventories. Here, remotely sensed measurements are frequently used as auxiliary data that enable the generation of wall-to-wall estimates of forest inventory attributes, thus providing maps of key elements of forest structure across the entire area of interest. In particular, high-resolution canopy height models (CHMs) can be valuable auxiliary datasets for this kind of application.

Canopy height measurements from airborne laser scanning (ALS) have been used successfully in operational forest management inventories in different countries, e.g. in Norway (NÆSSET 2014), Finland (MALTAMO & PACKALEN 2014), and Canada (WOODS et al. 2011). The most commonly used method for modelling forest inventory attributes is the area-based approach (NÆSSET 2002a). For this purpose, height and density metrics describing the vertical distribution of ALS returns are related to measurements at field plots in order to train predictive models for subsequent wall-to-wall mapping. Both parametric and non-parametric approaches can be used in such modelling efforts, e.g. linear regressions (MEANS et al. 2000), the *k*-most similar neighbours method (PACKALEN & MALTAMO 2007), or random forest (YU et al. 2010). As forest management planning can benefit from species-specific data, PACKALEN & MALTAMO (2007) combined ALS data with aerial photographs to generate area-based predictions separately for Scots pine, Norway spruce and broadleaved trees (as a group) for a managed boreal forest in Finland. A general introduction to area-based predictions using ALS and field plot data is given in NÆSSET (2014).

According to WHITE et al. (2013a) there has been a growing interest in alternative technologies capable of mapping surface heights over large areas, and image-based digital surface models (DSMs) have emerged as a suitable substitute for ALS-based DSMs (WHITE et al. 2015). Ongoing improvements in camera technology, as well as enhanced algorithms for image matching such as Semi-Global Matching (SGM; HIRSCHMÜLLER 2008) have provided further stimulus for these developments (HAALA & ROTHERMEL 2012). Currently, digital aerial photogrammetry (DAP) is viable for practical forestry applications in Germany and several other European countries, since aerial photographs are updated regularly by the surveying authorities, e.g. in two- or three-year cycles in Germany (STRAUB & SEITZ 2014) or a maximum of six-year cycles in Switzerland (GINZLER & HOBI 2015). In contrast, ALS data are currently not updated on a regular basis by the surveying authorities.

As image-based height measurements are limited to the outer ‘envelope’ of the forest canopy, additional detailed information about the topography is a basic prerequisite for calculating vegetation heights above ground. Here, pre-existing ALS-based digital terrain models (DTMs) can be used to

normalize the photogrammetric measurements. With respect to utilizing DAP for practical forestry applications in Germany, availability of the required ALS-based DTMs is not a limitation, since most surveying authorities have already produced DTMs based on ALS data for extensive areas, e.g. a 1 m-DTM is available for the entire state of Bavaria (LDBV 2015a).

The computation of surface models from aerial photographs has been studied for many years. In the study of ADLER & KOCH (1999) an automatically generated surface model was compared to manually measured elevation points for a spruce-dominated stand in southern Germany. It was found that the automatically generated surface model had a similar reliability as the manually measured height values. Several studies, conducted in Germany, Norway, and Finland, have assessed the direct estimation of stand heights from surface models derived from scanned aerial photographs (KÄTSCH & STÖCKER 2000, NÆSSET 2002b, KORPELA & ANTTILA 2004). In these studies, it was observed that, on average, stand heights were underestimated. To decrease this bias, NÆSSET (2002b) suggested a calibration with field data. KÄTSCH & STÖCKER (2000) mentioned the difficulty to obtain reliable height measurements of the terrain (bare Earth) from the aerial photographs. As possible solution to this problem, ST-ONGE et al. (2004) proposed a normalization of photogrammetric tree height measurements with an ALS-based DTM. Moreover, ST-ONGE et al. (2008) compared CHMs derived from DAP (normalized with an ALS-based DTM) to purely ALS-based CHMs. The authors concluded that height metrics derived from both types of CHMs were generally highly correlated.

More recent studies have compared the capability of using canopy height data obtained from DAP in conjunction with an ALS-based DTM to the use of purely ALS-based height data for the area-based estimation of forest inventory attributes. Most of these studies were carried out in conifer-dominated boreal forests, e.g. in Finland (NURMINEN et al. 2013, VASTARANTA et al. 2013), in Norway (RAHLF et al. 2014, GOBAKKEN et al. 2015), and in northeastern Ontario, Canada (PITT et al. 2014). Generally, the aforementioned studies have confirmed the applicability of image-based height measurements as an alternative to ALS data for the prediction of forest attributes such as mean height, mean diameter, total volume, total biomass or basal area, although root-mean-squared errors (*RMSEs*) were frequently slightly higher for DAP. Additionally, as stated e.g. by VASTARANTA et al. (2013), DAP lacks the penetration into the sub-canopy, and thus is disadvantageous to ALS when characterizing the vegetation density.

Similarly, WHITE et al. (2015) investigated the modelling performance of both DAP and ALS for a complex coastal temperate rainforest on Vancouver Island, Canada; and STRAUB et al. (2013) compared DAP and ALS in a mixed central European test site dominated by double and multi-layered stands in south-eastern Bavaria, Germany. Both studies affirmed the general finding that DAP is a suitable alternative for modelling forest inventory attributes, but the *RMSEs* reported for both ALS and DAP exceeded those obtained in the boreal test sites previously mentioned, though to a minor extend. Several factors might have influenced the modelling performances in the above-mentioned studies: the aerial camera systems, the photogrammetric software packages used for image matching, the size of the field plots, the modelling approaches, and the validation techniques used. Nevertheless, we assume that the differences in *RMSEs* observed for the aforementioned studies can be largely attributed to the different forest types and structures in the different test sites. As described by NÆSSET (2002b), the forest structure might even influence the performance of the image matching itself. He speculated that matching performs better for dense, even-aged broadleaved stands with rounded crowns compared with more heterogeneous coniferous stands with peaked crowns.

Thus, the present study was designed to explicitly evaluate the potential impact of the prevailing forest type on the modelling of forest attributes in central European forests. For this objective, we adopted a workflow developed in previously published work (STRAUB et al. 2013, STEPPER et al. 2015). In the work presented here, this workflow is verified under practical conditions in both a beech- and a spruce-dominated test site, which represent common broadleaf- and conifer-dominated forest environments in Germany (THÜNEN-INSTITUT 2015). As the abovementioned studies conducted in central European forests have focussed on the prediction of basal area and timber volume, there is still a need to test how accurately other attributes can be estimated. Thus, we evaluated models for a set of five different forest inventory attributes – stem density, basal area, quadratic mean diameter, volume, and Lorey's mean height.

## 2 Materials

### 2.1 *Test Sites*

For this study, we selected two test sites (Spessart 49° 57' N, 9° 24' E and Frankenwald, 50° 21' N, 11° 27' E) in the northern part of Bavaria, Germany, because the relative stocking of the species, present in each of the two test sites, represent common forest types in Germany, i.e., the beech and the spruce types (which cover 16.6% and 29.3% of the total forest area in Germany, respectively; THÜNEN-INSTITUT 2015). Tab. 1 summarizes the total size, the extent of the state forests, the topography, and the main tree species proportions at each site. In the Spessart area, European beech (*Fagus sylvatica* L.) is the dominant tree species on mesic sites, while dryer sites contain a higher proportion of sessile oak (*Quercus petraea* (Mattuschka) Liebl.). In the Frankenwald test site, the forests are mainly dominated by Norway spruce (*Picea abies* (L.) H. Karst.).

**Tab. 1:** Summary of the topography and main tree species at the Spessart and Frankenwald test sites; tree species proportions were calculated based on the respective basal areas at the forest inventory plots.

| **Test site** | **Spessart** | **Frankenwald** |
|---|---|---|
| Total size (ha) | 20824 | 15139 |
| State forest area (ha) | 8440 | 3821 |
| Elevation range (m a.s.l.) | 230 – 587 | 367 – 723 |
| Elevation average (m a.s.l.) | 418 | 580 |
| Forest type | beech-dominated | spruce-dominated |
| Tree species: | | |
| Norway spruce (%) | 9 | 78 |
| Scots pine (%) | 1 | 0 |
| other conifers (%) | 8 | 4 |
| European beech (%) | 56 | 14 |
| Sessile oak (%) | 24 | 0 |
| other broadleaves (%) | 2 | 4 |

### 2.2 *Forest Inventory Data*

Field measurements from regularly conducted forest management inventories of the BaySF served as training data for the modelling. NEUFANGER (2011) provides a concise outline of how forest management inventories in the state forests of Bavaria are planned and conducted. These inventories make use of three concentric sampling circles, as described in detail in STRAUB et al. (2013) and STEPPER et al. (2015). A general introduction to the use of concentric sample plots for forest inventories can be found in VAN LAAR & AKÇA (2007). Here, the trees are recorded in dependency of their diameter at breast height (measured 1.3 m above ground) and their distance to the plot centre. Whilst in the innermost circle with a radius of 2.82 m (25 m²) all trees are measured, the minimum diameter for inclusion is 30 cm in the largest circle with a radius of 12.62 m (500 m²). This 500 m² circle represents the reference area for the analysis of the remote sensing data in this study.
Permanent field plots were distributed systematically across the state forests in both test sites based on a regular 200 m × 200 m grid. In the Spessart test site, the terrestrial measurements used in this analysis were carried out from May to September 2011; while in the Frankenwald test site, sampling took place between April and September 2014. The plot centres were located using a Trimble GeoExplorer XT GPS device (maximum deviations of ±3–5 m; H. GRÜNVOGEL, personal communication, 4 August 2014). Within each circular plot, several characteristics such as species, diameter at breast height $d$, and tree height $h$ were recorded for individual trees. For our examination, we considered only trees with $d \geq 7$ cm, i.e., those trees that exceed the threshold for merchantable timber. Due to the concentric sampling method used, a different weight $w_i$ is applied to each measured value for each tree when computing per-hectare inventory attributes, which is related to the size of the concentric circle with radius $r$ (m) in which the tree was measured: $w_i = 10000/(\pi\, r^2)$.

The following attributes were computed for each of the field plots (where $m$ is the number of trees measured at the respective plot):

- Stem density *N*: Number of trees per hectare;

$$N\ (\text{trees ha}^{-1}) = \sum_{i=1}^{m} w_i \tag{1}$$

- Basal area *G* per hectare: Sum of the basal areas $g_i$, i.e., cross-sectional areas measured at 1.3 m above ground, of the trees measured multiplied by their respective weights;

$$G\ (\text{m}^2\text{ha}^{-1}) = \sum_{i=1}^{m} g_i\, w_i \tag{2}$$

- Quadratic mean diameter *QMD*;

$$QMD\ (\text{cm}) = \sqrt{\frac{\sum_{i=1}^{m} {d_i}^2 w_i}{\sum_{i=1}^{m} w_i}} \tag{3}$$

- Volume *V* per hectare: Sum of the single tree stem volumes $v_i$ multiplied by their respective weights;

$$V\ (\text{m}^3\text{ha}^{-1}) = \sum_{i=1}^{m} v_i\, w_i \tag{4}$$

- Lorey's mean height $H_L$: Weighted mean height, where each single tree height $h_i$ is weighted by the basal area $g_i$, multiplied by its respective weight;

$$H_L(\text{m}) = \frac{\sum_{i=1}^{m} h_i g_i w_i}{\sum_{i=1}^{m} g_i w_i} \tag{5}$$

This set of forest inventory attributes was computed for a total of 2010 field plots in the Spessart test site and 801 plots in the Frankenwald test site. Tab. 2 lists descriptive statistics for each of these attributes for the two test sites. In addition, statistics of the mean age, as derived from overstorey trees, i.e., those trees forming the upper canopy layer, are shown in Tab. 2.

**Tab. 2:** Descriptive statistics for the forest inventory attributes (stem density *N*, basal area *G*, quadratic mean diameter *QMD*, volume *V*, and Lorey's mean height $H_L$) derived from field plot observations (*n* = number of field plots with trees exceeding the minimum threshold $d \geq 7$ cm). In addition, statistics of the mean age of overstorey trees are shown.

| | Forest attribute | Min. | 1st quartile | Median | 3rd quartile | Max. | Mean | SD |
|---|---|---|---|---|---|---|---|---|
| Spessart beech-dominated (n = 2010) | *N* (trees ha$^{-1}$) | 19 | 182 | 385 | 906 | 4313 | 687 | 759 |
| | *G* (m² ha$^{-1}$) | 1 | 20 | 27 | 35 | 91 | 28 | 11 |
| | *QMD* (cm) | 8 | 20 | 31 | 42 | 94 | 32 | 15 |
| | *V* (m³ ha$^{-1}$) | 2 | 196 | 288 | 393 | 1228 | 304 | 158 |
| | $H_L$ (m) | 4 | 22 | 28 | 32 | 45 | 27 | 7 |
| | *Age* (years) | 12 | 52 | 106 | 150 | 378 | 108 | 59 |
| Franken-wald spruce-dominated (n = 801) | *N* (trees ha$^{-1}$) | 20 | 225 | 404 | 765 | 2997 | 587 | 550 |
| | *G* (m² ha$^{-1}$) | 2 | 18 | 30 | 39 | 86 | 29 | 15 |
| | *QMD* (cm) | 8 | 21 | 31 | 40 | 68 | 31 | 12 |
| | *V* (m³ ha$^{-1}$) | 1 | 147 | 296 | 409 | 846 | 288 | 174 |
| | $H_L$ (m) | 3 | 21 | 27 | 30 | 41 | 24 | 8 |
| | *Age* (years) | 8 | 49 | 63 | 81 | 157 | 65 | 26 |

### 2.3 *Remote Sensing Data*

All remote sensing data used in this study were acquired as a part of regular programs conducted by the Bavarian Administration for Surveying. Currently, aerial photographs are updated every three years in Bavaria. The general specifications for these official aerial photographs are provided in LDBV (2015b). An UltraCamXp camera was used in both test sites to acquire the stereo photography used in this analysis. The aerial survey covering the Spessart test site was conducted on 6 August 2011, while the aerial photographs for the Frankenwald test site were acquired in two separate flights – on 21 May and 8 June 2014. The forward and side overlaps of the images were 75% and 25% for the Spessart area and 75% and 40% for the Frankenwald area, resulting in a total of 122 and 210 stereo images, respectively. We used the panchromatic (PAN) images, with 12 bit radiometric resolution and a ground sampling distance of 0.20 m. The interior and exterior orientation parameters were provided by the vendor.

Moreover, we used the most recent ALS-based terrain models available – 1 m spatial resolution DTMs derived from topographic mapping surveys conducted by the Bavarian Administration for Surveying. These surveys were carried out in 2007 (last return point density: 2.83 m$^{-2}$) in the Spessart area and in 2009 (1.81 m$^{-2}$) in the Frankenwald area.

## 3 Methods

The main processing steps of our analysis described in the section that follows are:

- Computation of canopy height models (CHMs)
- Calculation of predictor variables based on the CHMs calculated in step one.
- Area-based modelling of forest inventory attributes using random forest with built-in recursive feature elimination.

### 3.1 *Computation of Canopy Height Models*

For dense image matching of the PAN-images, we used the SGM approach, as implemented in the Remote Sensing Software Package Graz (RSG, v. 7.46; JOANNEUM RESEARCH 2014). Within SGM,

the dissimilarity between corresponding pixels in two epipolar images – the base and match image – is measured by matching costs, i.e., the aggregation of the costs calculated along each 45° 1D search path from the respective base image pixel (HIRSCHMÜLLER 2008). For each base image pixel, the disparity that corresponds to the minimum aggregated costs is selected, and a disparity map for the stereo pair is computed. In RSG, disparities are computed twice for each stereo pair, by switching the role of base and match image. Using a threshold for maximum disparity differences, consistency of the matching can be checked and mismatches can be eliminated (GEHRKE et al. 2010). According to the recommendations of the software developers of RSG with regard to the imagery available, we set the parameters for both test sites as follows: the maximum back-matching threshold was defined as 1.5 pixels, the number of image pyramid levels was set to 4, and the matching step-size at the final pyramid level was set to 1 pixel. All stereo pairs from the along-track overlap (min. 60 %) were used; across-track stereo pairs were not considered due to the small area of across-track overlap between the aerial images acquired. Based on the resulting point clouds, DSMs (1 m spatial resolution) were derived using the point triangulation method as implemented in the las2dem tool from LAStools (v. 141218; RAPIDLASSO GMBH 2015). Finally, to derive canopy heights above ground, the surface heights were normalized by subtracting the height values from the existing ALS-based DTMs described above from the heights of the DSMs.

### 3.2 *Calculation of Predictor Variables Based on the CHMs*

To derive predictor variables from the CHMs, we developed a routine based on the machine vision software HALCON (v. 12.0.1; MVTEC SOFTWARE GMBH 2015). Following the recommendations of WHITE et al. (2013b) for ALS data, we calculated the following 14 predictors related to forest height, canopy cover and variability in height for each 500 m² inventory plot region:

- Six height metrics: minimum $h_{min}$, first quartile $h_{25}$, mean $h_m$, median $h_{50}$, third quartile $h_{75}$, and maximum $h_{max}$.
- Six canopy cover (*cc*) metrics as indicators for vegetation density: $cc_0$, $cc_1$, … , $cc_6$. Crown regions *cr* were extracted based on six different height thresholds (2 m, 5 m, 10 m, 15 m, 20 m, and 25 m) and related to the total plot area: $cc\ (\%) = area(cr)/area(plot) \times 100$.
- Two canopy height variability metrics: standard deviation $h_{sd}$ and coefficient of variation $h_{cv}$.

### 3.3 *Area-based Forest Attribute Modelling*

We used the open-source statistical software R (v. 3.2.2; R CORE TEAM 2015) for the development of the modelling procedure. The prediction models were implemented using the R packages *randomForest* (LIAW & WIENER 2002) and *caret* (KUHN 2015). Random forest was used as modelling approach, since it was successfully applied in several other studies dealing with the estimation of forest attributes using remotely sensed data (e.g. PITT et al. 2014, WHITE et al. 2015, IMMITZER et al. 2016). The main characteristics of random forest, as developed by BREIMAN (2001), are:

- Multiple base learners – the decision trees – are trained based on bootstrap-sampled versions of the training data. Generating bootstraps, i.e., random subsets of the entire set of training data, introduces a first random component in the tree-building process (KUHN & JOHNSON 2013). To obtain the prediction for new samples, the predictions of the individual decision trees are averaged.
- During the decision tree construction process, at each split, a random subset of predictor variables to choose from is selected. This second term of randomness helps decorrelate the individual decision trees, thus improving the overall performance of the estimator (HASTIE et al. 2009).

As suggested by KUHN & JOHNSON (2013), we set the parameter $n_{tree}$ = 1000, i.e., an ensemble of 1000 trees was used to build the respective forests. The number of variables randomly selected at each split was set to one-third of the number of available predictors ($m_{try} = p/3$), as recommended by BREIMAN (2001). Besides the coefficient of determination ($R^2$), we computed the root-mean-squared error (*RMSE*) and the *bias* as quantitative measures for model performance. In order to achieve reliable estimates for these measures, we applied a 10-fold cross-validation repeated five times (KUHN & JOHNSON 2013). Thus, 50 different held-out sets (from here on referred to as folds, *f*) were used to assess the model outcomes for each of the five forest inventory attributes at each of the two test sites.

For each fold, we computed the $RMSE_f$ and $bias_f$, (6) and (7). As per STEPPER et al. (2015), these $RMSE_f$ and $bias_f$ values were averaged over the 50 folds to generate overall measures for *RMSE* and *bias*, (8) and (9). In the same way, overall $R^2$ measures were derived as the average of the $R^2_f$ values from the 50 folds (10), where each $R^2_f$ value corresponded to the squared Pearson's correlation coefficient between the predicted and observed values in the respective fold *f*.

$$RMSE_f = \sqrt{\frac{\sum_{i=1}^{n}(y_i - \hat{y}_i)^2}{n}} \quad (6)$$

$$bias_f = \frac{\sum_{i=1}^{n}(y_i - \hat{y}_i)}{n} \quad (7)$$

$$RMSE = \frac{\sum_{j=1}^{k} RMSE_{f,j}}{k} \quad (8)$$

$$bias = \frac{\sum_{j=1}^{k} bias_{f,j}}{k} \quad (9)$$

$$R^2 = \frac{\sum_{j=1}^{k} R^2_{f,j}}{k} \quad (10)$$

In (6) to (10), $y_i$ refers to the observed value, $\hat{y}_i$ is the predicted value of the $i^{\text{th}}$ of $n$ sampled observations in one of the $k$ folds *f*.

Predictors derived from image-based CHMs can be highly prone to multi-collinearity (WHITE et al. 2015). Despite the ability of random forest to handle high-dimensional and highly correlated predictor datasets, IMMITZER et al. (2016) demonstrated that an additional step implementing feature selection resulted in improved model performance when estimating timber volume based on WorldView-2 stereo satellite data. Accordingly, we applied recursive feature elimination (RFE) as implemented in the *caret* package. This search algorithm utilizes the feature importance of random forest – as computed for the full model including all 14 predictors – to sequentially remove each predictor based on its importance. For each new predictor subset created by removing the next sequential predictor, new models are trained and the respective *RMSEs* are stored. Finally, the best performing subset is determined by the lowest *RMSE*. Comprehensive explanations regarding RFE and its implementation in *caret* are provided in KUHN & JOHNSON (2013) and KUHN (2013).

## 4 Results

For each of the forest inventory attributes considered here (*N*, *G*, *QMD*, *V*, and $H_L$), we generated individual random forest models separately for each of the two test sites – Spessart and Frankenwald. The RFE implemented in the *caret* package selected different numbers of predictors for the individual random forest models ranging from 5 to 14. For eight of the developed models the RFE selected a combination of height, canopy cover and canopy height variability metrics. For all models, a height metric achieved the highest importance score. In both test sites, $h_{50}$ was ranked as the most important predictor for *V*. Moreover, $h_{max}$ was ranked as the most influential predictor for *N*, *QMD* and $H_L$ in both sites.

The cross-validated estimates for $R^2$, *RMSE* and *bias* are summarized in Tab. 3. As is common practice, the absolute *RMSE* and *bias* values were 'normalized' by dividing by the mean of the observations, hereafter referred to as $RMSE_{mean}$ (%) and $bias_{mean}$ (%). Moreover, we used the median for 'normalization' (see Tab. 2), referred to as $RMSE_{median}$ (%) and $bias_{median}$ (%).

Overall, the $R^2$ values of the models for the different forest attributes in both test sites varied in the range from 0.26 to 0.84. For the attributes *G*, *QMD*, *V*, and $H_L$, higher $R^2$ values were obtained for the spruce-dominated Frankenwald, whereas for *N* the model for the beech-dominated Spessart resulted in a higher $R^2$. As expected, highest $R^2$ values were achieved for $H_L$ in both test sites. The *G* model developed for the beech-dominated forest yielded the lowest $R^2$.

For all models, the resulting *RMSEs* were consistently smaller than the corresponding standard deviations of the observations (Tab. 2). For $H_L$, the $RMSE_{mean}$ (%) values for the spruce- and the beech-dominated test sites were identical, and the $RMSE_{median}$ (%) values were very close. Furthermore, with respect to the $RMSE_{mean}$ (%), the predictions were similar for *N* and *G* in the two test sites. For *V* and *QMD*, lower *RMSEs* were obtained for the spruce-dominated forest, with more evident differences for the *QMD*.

Within the test sites, both options for normalization (i.e., $RMSE_{mean}$ (%) and $RMSE_{median}$ (%)) resulted in similar relative *RMSEs* for the attributes *G*, *QMD*, *V* and $H_L$, whereas major differences occurred for *N*. Due to the heavily right-skewed distributions of the observed field data for *N* (see Tab. 2), using the median for normalization resulted in much higher numbers compared to the normalization by the mean.

*Bias* was small for all random forest models generated. Minor systematic overpredictions were only observed for the models describing stem density *N*.

The scatter of predicted vs. observed values for all attributes is shown by hexagonal binning plots in Fig. 1. Additionally, the distributions of model residuals, i.e., differences of observed minus predicted values, were computed for distinct age classes which are commonly used in forest management practice in Germany (I = 1–20 years, II = 21–40, III = 41–60, … , X = 181–200; KRAMER & AKÇA 2008). The residual distributions are displayed in Fig. 2 and the following main observations can be made:

- For *N*, a large scatter of residuals is visible for the younger age classes (especially for the classes I to III), which is similar for both test sites. Nonetheless, the medians are close to zero.
- For *G* and *V*, the boxplots indicate a slight overprediction for the youngest age class I, whereas the models tended to underpredict in the oldest class, i.e., >X for Spessart and >VI for Frankenwald.
- For *QMD*, the distribution of the residuals widens with increasing age in both test sites. Moreover, the models obviously overpredicted *QMDs* at inventory plots with age class I. Furthermore, the *QMD* model for the Spessart test site showed a tendency to underpredict *QMDs* in older age classes (especially in the classes IX, X and >X).
- For $H_L$, the models overpredicted the observed values in age class I in both test sites. In addition, the boxplots for the Spessart test site indicate that $H_L$ was obviously underpredicted in the oldest age class >X.

**Tab. 3:** Cross-validated measures of model performance ($R^2$, *RMSE*, *bias*) of the random forest models for stem density *N*, basal area *G*, quadratic mean diameter *QMD*, volume *V*, and Lorey's mean height $H_L$, calculated separately for the two test sites/forest types Spessart and Frankenwald; the absolute *RMSE* and *bias* values were 'normalized' with the mean and the median of the observations.

| | **Forest attribute** | $R^2$ | ***RMSE*** | $RMSE_{mean}$ **(%)** | $RMSE_{median}$ **(%)** | ***bias*** | $bias_{mean}$ **(%)** | $bias_{median}$ **(%)** |
|---|---|---|---|---|---|---|---|---|
| Spessart, beech-dominated ($n$ = 2010) | $N$ (trees ha$^{-1}$) | 0.60 | 483 | 70.3 | 125.4 | -4 | -0.6 | -1.1 |
| | $G$ (m² ha$^{-1}$) | 0.26 | 9.9 | 36.0 | 36.7 | -0.1 | -0.2 | -0.2 |
| | *QMD* (cm) | 0.52 | 10.4 | 32.3 | 33.7 | -0.2 | -0.5 | -0.5 |
| | $V$ (m³ ha$^{-1}$) | 0.47 | 114.9 | 37.8 | 39.9 | -0.9 | -0.3 | -0.3 |
| | $H_L$ (m) | 0.79 | 3.3 | 12.4 | 11.9 | 0.0 | -0.1 | -0.1 |
| Frankenwald, spruce-dominated ($n$ = 801) | $N$ (trees ha$^{-1}$) | 0.37 | 440 | 74.9 | 108.8 | -8 | -1.3 | -1.9 |
| | $G$ (m² ha$^{-1}$) | 0.54 | 10.3 | 35.2 | 34.4 | 0.0 | 0.0 | 0.0 |
| | *QMD* (cm) | 0.61 | 7.6 | 24.9 | 24.3 | 0.0 | -0.1 | -0.1 |
| | $V$ (m³ ha$^{-1}$) | 0.70 | 96.1 | 33.3 | 32.5 | -0.3 | -0.1 | -0.1 |
| | $H_L$ (m) | 0.84 | 3.0 | 12.4 | 11.3 | 0.0 | 0.1 | 0.1 |

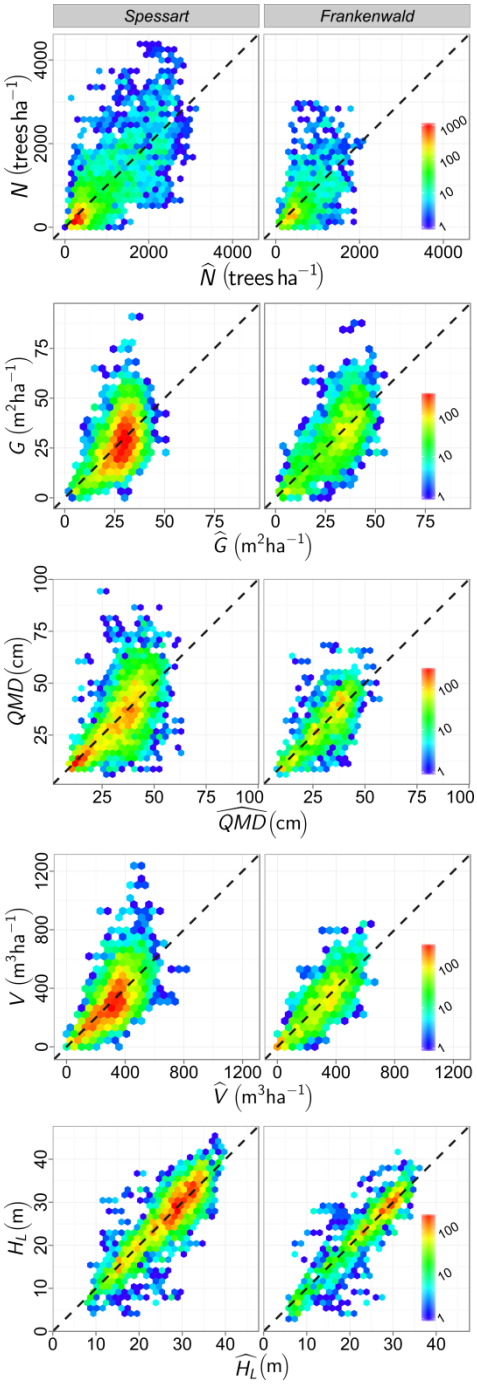


411

412 **Fig. 1:** Predicted (x-axis) vs. observed (y-axis) values for stem density *N*, basal area *G*,
413 quadratic mean diameter *QMD*, volume *V,* and Lorey's mean height $H_L$, shown as
414 hexagonal binning plots (xy-plane tessellated by a regular grid of hexagons; hexagons are
415 coloured according to the number of points falling into each hexagon; LEWIN-KOH 2011).

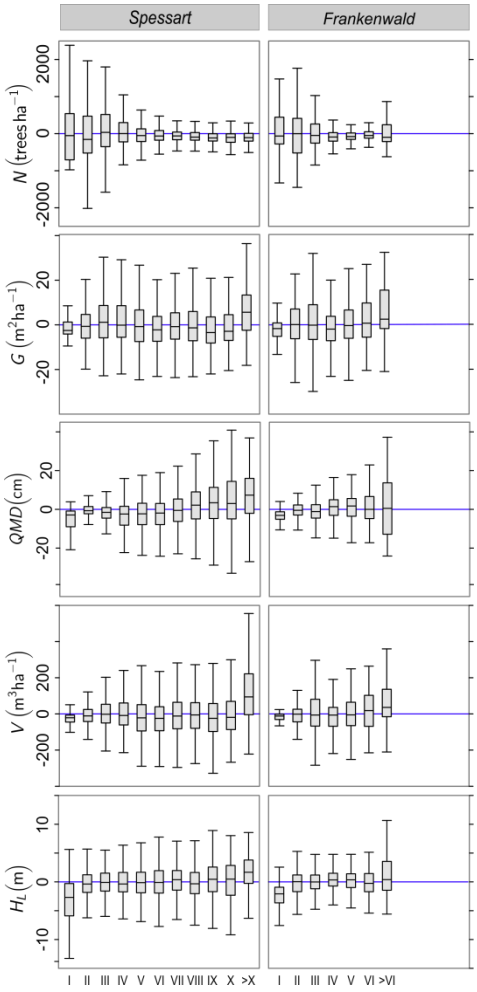


**Fig. 2:** Distributions of residuals (observed minus predicted values) for the prediction of stem density *N*, basal area *G*, quadratic mean diameter *QMD*, volume *V,* and Lorey's mean height $H_L$, separately for 20-year age classes.

## 5 Discussion

The $R^2$ values for *G*, *QMD*, *V* and $H_L$ achieved for the spruce-dominated Frankenwald revealed a better model fit ($R^2$: 0.54, 0.61, 0.70, 0.84) compared to those for the beech-dominated Spessart ($R^2$: 0.26, 0.52, 0.47, 0.79). Moreover, with respect to the $RMSE_{mean}$ (%) values, a slightly higher level of accuracy was observed for the prediction of *QMD* for the spruce-dominated forest type. According to NIKLAS (1994) and PRETZSCH et al. (2013) this observation might be partially attributed to the allometric difference in the height-diameter-relationships of conifers and broadleaved tree species. Moreover, it has to be considered that the CHMs from DAP mainly characterize the overstorey and do not include information about the understorey structure, which is not visible in the aerial photographs. Thus, it must be expected that reference trees growing in the understorey add some additional scatter to predictive models. We assume that this influence can vary for spruce- and beech-dominated forests, due to differences in stand structures. For assessing the understorey, ALS

technology is advantageous as it penetrates through small gaps in the canopy and may provide additional returns from underlying vegetation layers (WHITE et al. 2013a).

The plot-level $RMSE_{mean}$ (%) values obtained for *V* and *G* in the present study were similar to those values reported by STRAUB et al. (2013) for a mixed managed forest in southern Bavaria (37.9% for *V* and 35.3% for *G*). Frequently, better accuracies were reported for managed conifer-dominated boreal test sites which are most probably due to more homogeneous forest structures in contrast to the more diverse central European forest conditions. As an example, NURMINEN et al. (2013) applied random forest for a test site in Finland and achieved normalized *RMSEs* of 6.8% for mean height, 12.0% for mean diameter and 22.6% for volume based on UltraCamD images with a forward overlap of 80%. Moreover, VASTARANTA et al. (2013), who applied random forest within a nearest neighbour search for a test site in Finland, reported *RMSEs* of 11.2% for mean height, 21.7% for mean diameter, 23.6% for basal area, and 24.5% for volume when using UltraCamXp data with a forward overlap of 70%.

As in the study of Woods et al. (2011), who used ALS data for an operational forest inventory in boreal Ontario, we obtained poorest model accuracies, i.e., largest *RMSEs*, for *N* in comparison to the other tested attributes. As mentioned above, trees in the understorey cannot be captured by DAP. Most likely, this fact contributed to the large *RMSEs* for *N*. Moreover, it was shown for *N*, with a heavily skewed distribution of the observed values that the two variants for normalizing the absolute *RMSEs* resulted in very different values in the two test sites. Thus, for this type of data, we suggest that the *RMSEs* normalized by the median give a more robust estimate of the relative *RMSE*.

For several attributes, e.g. for *G* and *V* in both test sites, the models overpredicted the ground measured values at inventory plots from the youngest age class, and vice-versa underpredicted in the oldest age classes. This may be partly explained by the fact that random forest tends to overpredict low values and to underpredict high ones which was stated in several publications, e.g. BACCINI et al. (2004), VANSELOW & SAMIMI (2014), or IMMITZER et al. (2016). This is also reflected by the scatterplots shown in Fig. 1. Moreover, the underpredictions in the oldest age classes seem plausible, since the functional relationship between canopy height and the actual stocking (*G* or *V*) will be weaker for older forest stands with a decreasing vertical growth. Additionally, as we observed for our data, the distribution of residuals is related to the variability of the observations within the respective age classes. For example, for both test sites, a larger scattering of residuals was revealed for *N* in the young age classes, which is associated with the expected larger variability and range of stem densities for these classes compared to the lower variabilities in older classes.

We applied random forest regression within R and our results confirmed the suitability of this modelling approach. In previous studies, PENNER et al. (2013) and STEPPER et al. (2015) showed that random forest produced accuracies comparable to parametric models. Random forest has several advantages for operational applications, e.g.: a priori assumptions about the relationship between response and predictor variables are not required, multicollinearity among predictors can be handled, and large numbers of predictors can be considered without overfitting (PITT et al. 2014, IMMITZER et al. 2016). Still, disadvantages of the random forest regression, that are frequently considered, are the 'black-box' nature of the algorithm (WHITE et al. 2013b) as well as the inability – common to all non-parametric approaches – to extrapolate beyond the range of the training data (STEPPER et al. 2015). Thus, in order to train prediction models that are valid for the entire population, samples that cover the complete range of existing values are necessary. Since many sample plots were distributed on a dense grid in both test sites of this study, we assume that a good coverage is guaranteed. Besides the representativeness of the sample, the size and the georeferencing accuracy of the field plots will have an influence on the predictive power of the models (WHITE et al. 2013b). Thus, we attribute a part of the shown scatter between observed and predicted values to the reported 3 m – 5 m GPS offsets of the plot positions. As described in section 2.2, each field plot consists of three concentric sampling circles. This plot design is commonly used for the forest management inventories in the state forests of Bavaria as well as in other federal states in Germany. According to LAWRENCE et al. (2010), the fundamental advantage of concentric circles is that the more frequent small trees are measured within small circles and the less frequent large trees are measured in large circles. This practice reduces the overall costs of the field survey with just little loss in precision. However, the use of concentric circles as training data might have some impact on the area-based modelling, if the sample for the small trees is not representative for the largest circle which is commonly used as the reference area to extract remote sensing features.

As mentioned in the introduction, ALS was already integrated successfully into operational forest management inventories in some countries using the area-based approach. In principle, area-based predictions enable the production of wall-to-wall maps displaying the estimated spatial distribution of forest inventory attributes at a spatial resolution which relates to the size of the field plots used to train the model (WHITE et al. 2013b), i.e., 500 m² for our data. Using height information generated from dense image matching for the spatial prediction of forest attributes is the subject of ongoing research. Recently, we conducted a first pilot study together with forest inventory experts of the BaySF to assess the benefit of CHMs from DAP and derived wall-to-wall timber volume maps to support forest management tasks. The inventory experts determined several applications for these remote sensing products as a supplement to the existing terrestrial data. For example, CHMs were found to be useful to support and validate the manual delineation of management units, i.e., forest stand regions. Moreover, the inventory experts saw potential to derive aggregated volume estimates for stand regions based on the wall-to-wall timber volume maps, which currently cannot be deduced from the field data. This information might be useful to determine the harvest volume more exactly. In future, additional studies and investigations have to be conducted together with the end-users to further evaluate the potential and the limitations of DAP for practical forestry applications.

## 6 Conclusion

Following other studies, which have used DAP to model forest inventory attributes, we investigated the prediction of mean and total plot-level attributes. These predictions were compared for a beech- and a spruce-dominated central European test site. With respect to relative *RMSEs*, i.e., divided by the observation means, most distinct differences were observed for the prediction of *QMD* with a slightly better accuracy for the spruce-dominated forest, whereas similar outcomes were obtained for the other tested attributes. To better understand the influence of tree species on model performances, future research may focus on the assessment of species-specific models, e.g., to predict the plot-level volume of the main species for a selected test region using both height and spectral information from the aerial photographs.

We conclude that the proposed workflow can provide predictions for forest areas where terrestrial inventory data are available to train predictive models, such as the state forests of Bavaria. Conversely, for many small-parcelled private forest properties in Bavaria, no such terrestrial inventories are conducted. To additionally provide information for the forest management in these estates, further research might investigate the transferability of prediction models generated in state forests to other forest areas.

## Acknowledgements

The authors are grateful to the Bavarian State Forest Enterprise (BaySF) for supplying the inventory data and to the Bavarian Administration for Surveying for providing the remote sensing data used in this research. We also thank Prof. Dr. MATHIAS SCHARDT and Dr. KARLHEINZ GUTJAHR from JOANNEUM RESEARCH for assistance with and permission to use the RSG software, LAURA CARLSON for language editing and RUDOLF SEITZ for helpful comments on earlier drafts of this paper. We owe special thanks to the reviewers for thorough and excellent reviews which improved the manuscript. Funding of this research was granted by the Bavarian State Ministry of Food, Agriculture and Forestry.

## References

ADLER, P. & KOCH, B., 1999: Digital photogrammetry for forest ecosystem monitoring. – Conference Proceedings 'Remote Sensing and Forest Monitoring', Rogow, Poland.

BACCINI, A., FRIEDL, M.A., WOODCOCK, C.E. & WARBINGTON, R., 2004: Forest biomass estimation over regional scales using multisource data. – Geophysical Research Letters **31**, L10501.

BAYSF, 2015: Statistikband 2015, Bayerische Staatsforsten. – http://www.baysf.de/de/publikationen.html (7.3.2016).

BREIMAN, L., 2001: Random forests. – Machine learning **45** (1): 5–32.
GEHRKE, S., MORIN, K., DOWNEY, M., BOEHRER, N. & FUCHS, T., 2010: Semi-global matching: An alternative to LIDAR for DSM generation? – The International Archives of the Photogrammetry, Remote Sensing and Spatial Information Sciences XXXVIII – Part 1.
GINZLER, C. & HOBI, M., 2015: Countrywide stereo-image matching for updating digital surface models in the framework of the Swiss National Forest Inventory. – Remote Sensing **7** (4): 4343–4370.
GOBAKKEN, T., BOLLANDSÅS, O.M. & NÆSSET, E., 2015: Comparing biophysical forest characteristics estimated from photogrammetric matching of aerial images and airborne laser scanning data. – Scandinavian Journal of Forest Research **30** (1): 73–86.
HAALA, N. & ROTHERMEL, M., 2012: Dense Multi-Stereo Matching for High Quality Digital Elevation Models. – PFG – Photogrammetrie, Fernerkundung, Geoinformation **2012** (4): 331–343.
HASTIE, T., TIBSHIRANI, R. & FRIEDMAN, J.H., 2009: The elements of statistical learning. – Second edition, Springer, New York, NY, USA.
HIRSCHMÜLLER, H., 2008: Stereo processing by semiglobal matching and mutual information. – IEEE Transactions on Pattern Analysis and Machine Intelligence **30** (2): 328–341.
IMMITZER, M., STEPPER, C., BÖCK, S., STRAUB, C. & ATZBERGER, C., 2016: Use of WorldView-2 stereo imagery and National Forest Inventory data for wall-to-wall mapping of growing stock. – Forest Ecology and Management **359**: 232–246.
JOANNEUM RESEARCH, 2014: Remote Sensing Software Package Graz. http://www.remotesensing.at/en/remote-sensing-software.html (7.3.2016).
KÄTSCH, C. & STÖCKER, M., 2000: Untersuchungen zur automatischen Ermittlung von Bestandeshöhen auf Luftbildern mit Hilfe der Digitalen Photogrammetrie. – Allgemeine Forst- und Jagdzeitung **171**: 74–80.
KORPELA, I. & ANTTILA, P., 2004: Appraisal of the mean height of trees by means of image matching of digitised aerial photographs. – The Photogrammetric Journal of Finland **19** (1): 23–36.
KRAMER, H. & AKÇA, A., 2008: Leitfaden zur Waldmesslehre. – J.D. Sauerländer's Verlag, Frankfurt am Main.
KUHN, M. & JOHNSON, K., 2013: Applied Predictive Modeling. – Springer, New York, NY, USA.
KUHN, M. 2015: Package 'caret'. https://cran.r-project.org/web/packages/caret/caret.pdf (7.3.2016).
LAWRENCE, M., MCROBERTS, R.E., TOMPPO, E., GSCHWANTNER, T. & GABLER, K., 2010: Comparisons of National Forest Inventories. – TOMPPO, E., GSCHWANTNER T., LAWRENCE, M. & MCROBERTS, R.E. (eds.): National Forest Inventories. – Springer: 19–32.
LDBV, 2015a: Digitale Geländemodelle (DGM). Product information leaflet. http://vermessung.bayern.de/file/pdf/1614/download_faltblatt-dgm09.pdf (7.3.2016).
LDBV, 2015b: Luftbildprodukte. Product information leaflet. http://vermessung.bayern.de/file/pdf/1039/download_faltblatt-luftbilder08.pdf (7.3.2016).
LEWIN-KOH, N., 2011: Hexagon Binning: an Overview. https://cran.r-project.org/web/packages/hexbin/vignettes/hexagon_binning.pdf. (7.3.2016).
LIAW, A. & WIENER, M., 2002: Classification and Regression by randomForest. – R news **2** (3): 18–22.
MALTAMO, M. & PACKALEN, P., 2014: Species-specific management inventory in Finland. – MALTAMO, M., NÆSSET, E. & VAUHKONEN, J. (eds.): Forestry Applications of Airborne Laser Scanning: 241–252, Springer, Dordrecht, Netherlands.
MEANS, J.E., ACKER, S.A., FITT, B.J., RENSLOW, M., EMERSON, L. & HENDRIX, C.J., 2000: Predicting forest stand characteristics with airborne scanning LiDAR. Photogrammetric Engineering & Remote Sensing **66** (11): 1367–1371.
MVTEC SOFTWARE GMBH 2015: HALCON. http://www.halcon.com/ (7.3.2016).
NÆSSET, E., 2002a: Predicting forest stand characteristics with airborne scanning laser using a practical two-stage procedure and field data. – Remote Sensing of Environment **80** (1): 88–99.
NÆSSET, E., 2002b: Determination of mean tree height of forest stands by digital photogrammetry. – Scandinavian Journal of Forest Research **17** (5): 446–459.

596 NÆSSET, E., 2014: Area-based inventory in Norway – from innovation to an operational reality. –
597 MALTAMO, M., NÆSSET, E. & VAUHKONEN, J. (eds.): Forestry Applications of Airborne Laser
598 Scanning: 215–240, Springer, Dordrecht, Netherlands.
599 NEUFANGER, M., 2011: Richtlinie für die mittel- und langfristige Forstbetriebsplanung in den
600 Bayerischen Staatsforsten. – Forsteinrichtungsrichtlinie – FER 2011.
601 NIKLAS, K.J., 1994: Plant allometry. – University of Chicago Press, Chicago, IL, USA.
602 NURMINEN, K., KARJALAINEN, M., YU, X., HYYPPÄ, J. & HONKAVAARA, E., 2013: Performance of
603 dense digital surface models based on image matching in the estimation of plot-level forest
604 variables. – ISPRS Journal of Photogrammetry and Remote Sensing **83**: 104–115.
605 PACKALEN, P. & MALTAMO, M., 2007: The k-MSN method in the prediction of species specific stand
606 attributes using airborne laser scanning and aerial photographs. – Remote Sensing of
607 Environment **109** (3):328–341.
608 PENNER, M., PITT, D.G. & WOODS, M.E., 2013: Parametric vs. nonparametric LiDAR models for
609 operational forest inventory in boreal Ontario. – Canadian Journal of Remote Sensing **39** (5):
610 426–443.
611 PITT, D.G., WOODS, M. & PENNER, M., 2014: A Comparison of point clouds derived from stereo
612 imagery and airborne laser scanning for the area-based estimation of forest inventory attributes in
613 boreal Ontario. – Canadian Journal of Remote Sensing **40** (3): 214–232.
614 PRETZSCH, H., DAUBER, E. & BIBER, P., 2013: Species-specific and ontogeny-related stem allometry
615 of European forest trees: evidence from extensive stem analyses. – Forest Science **59** (3): 290–
616 302.
617 R CORE TEAM, 2015: The R project for statistical computing. – https://www.r-project.org/ (7.3.2016).
618 RAHLF, J., BREIDENBACH, J., SOLBERG, S., NÆSSET, E. & ASTRUP, R., 2014: Comparison of four types
619 of 3D data for timber volume estimation. – Remote Sensing of Environment **155**: 325–333.
620 RAPIDLASSO GMBH 2015: LAStools. – http://rapidlasso.com/lastools/ (7.3.2016).
621 STEPPER, C., STRAUB, C. & PRETZSCH, H., 2015: Using semi-global matching point clouds to estimate
622 growing stock at the plot and stand levels: application for a broadleaf-dominated forest in central
623 Europe. – Canadian Journal of Forest Research **45** (1): 111–123.
624 ST-ONGE, B., JUMELET, J., COBELLO, M. & VEGA, C., 2004: Measuring individual tree height using a
625 combination of stereophotogrammetry and lidar. – Canadian Journal of Forest Research **34** (10):
626 2122–2130.
627 ST-ONGE, B., VEGA, C., FOURNIER, R.A. & HU, Y., 2008: Mapping canopy height using a combination
628 of digital stereo-photogrammetry and lidar. – International Journal of Remote Sensing **29** (11):
629 3343–3364.
630 STRAUB, C., STEPPER, C., SEITZ, R. & WASER, L.T., 2013: Potential of UltraCamX stereo images for
631 estimating timber volume and basal area at the plot level in mixed European forests. – Canadian
632 Journal of Forest Research **43** (8): 731–741.
633 STRAUB, C. & SEITZ, R., 2014: Verwendungspotential von Fernerkundungsdaten in der
634 Forsteinrichtung. – Vortrag bei der Tagung der Arbeitsgemeinschaft Forsteinrichtung am
635 22.10.2014 in Weimar.
636 THÜNEN-INSTITUT, 2015: Dritte Bundeswaldinventur (2012). – https://bwi.info. (7.3.2016).
637 VAN LAAR, A. & AKÇA, A. 2007: Forest Mensuration. – Springer, Dordrecht, Netherlands.
638 VANSELOW, K.A. & SAMIMI, C. 2014: Predictive mapping of dwarf shrub vegetation in
639 an arid high mountain ecosystem using remote sensing and Random Forests. – Remote Sensing
640 **6**, 6709–6726.
641 VASTARANTA, M., WULDER, M.A., WHITE, J.C., PEKKARINEN, A., TUOMINEN, S., GINZLER, C.,
642 KANKARE, V., HOLOPAINEN, M., HYYPPÄ, J. & HYYPPÄ, H., 2013: Airborne laser scanning and
643 digital stereo imagery measures of forest structure: comparative results and implications to forest
644 mapping and inventory update. – Canadian Journal of Remote Sensing **39** (05): 382–395.
645 WHITE, J.C., WULDER, M.A., VASTARANTA, M., COOPS, N.C., PITT, D. & WOODS, M., 2013a: The
646 utility of image-based point clouds for forest inventory: A comparison with airborne laser
647 scanning. – Forests **4** (3): 518–536.
648 WHITE, J.C., WULDER, M.A., VARHOLA, A., VASTARANTA, M., COOPS, N.C., COOK, B.D., PITT, D.
649 & WOODS, M., 2013b: A best practices guide for generating forest inventory attributes from

airborne laser scanning data using an area-based approach. – Canadian Wood Fibre Centre, Victoria, BC, Canada. – http://cfs.nrcan.gc.ca/publications?id=34887 (7.3.2016).

WHITE, J., STEPPER, C., TOMPALSKI, P., COOPS, N. & WULDER, M., 2015: Comparing ALS and image-based point cloud metrics and modelled forest inventory attributes in a complex coastal forest environment. – Forests **6** (10): 3704–3732.

WOODS, M., PITT, D., PENNER, M., LIM, K., NESBITT, D., ETHERIDGE, D. & TREITZ, P., 2011: Operational implementation of a LiDAR inventory in Boreal Ontario. – The Forestry Chronicle **87** (4): 512–528.

YU, X., HYYPPÄ, J., HOLOPAINEN, M. & VASTARANTA, M., 2010: Comparison of area-based and individual tree-based methods for predicting plot-level forest attributes. – Remote Sensing **2** (6): 1481–1495.

Address of the Authors:

Dr. CHRISTOPH STRAUB, M.Sc. CHRISTOPH STEPPER, Bavarian State Institute of Forestry (LWF), Department of Information Technology, Hans-Carl-von-Carlowitz-Platz 1, D-85354 Freising, Tel: +49(0)8161-71-5875, Fax: +49(0)8161-71-4971, e-mail: {christoph.straub}, {christoph.stepper}@lwf.bayern.de

Manuskript eingereicht: Dezember 2015
Angenommen: April 2016